STM study of step dynamics around a bulk dislocation intersection with a Ag(111) surface

Karina Morgenstern,[1] Erik Lægsgaard,[2] and Flemming Besenbacher[2]

[1]*Institut für Festkörperphysik, Universität Hannover, Applestr. 2, D-30167 Hannover, Germany*

[2]*Interdisciplinary Nanoscience Center (iNANO) and Department of Physics and Astronomy, University of Aarhus, DK-8000 Aarhus C, Denmark*

(Received 27 April 2004; revised manuscript received 25 October 2004; published 29 April 2005)

The atomic-scale dynamics of a helical step emerging at the intersection of a bulk dislocation with the Ag(111) surface has been studied by scanning tunneling microscopy. The helix is found to unroll, thereby forcing a step to pass the intersection region. A coalescence event creates a situation far from equilibrium, which influences the transition of the helix towards an equilibrium structure. The evolution following the coalescence differs qualitatively from the coalescence of vacancy islands. A model is tentatively proposed, which explains the observed changes in the decay rates of the dislocation.

Defects and imperfections are of utmost importance for the understanding of phenomena within the area of nanoscience and materials science. Especially the dislocations that mark the border between the displaced and nondisplaced parts of a crystal play a central role in the mechanical properties of crystalline solids.[1] A bulk dislocation which intersects the surface of a crystal will result in a surface step that ends at the dislocation, if the Burgers dislocation vector has a nonzero component along the surface normal. Such dislocation-induced steps play a significant role in a number of surface-related phenomena, such as nucleation and growth and the dynamic approach towards thermodynamically stable structures. For example, the Ehrlich-Schwoebel barrier,[2] which hinders interlayer mass transport, can be circumvented by atom diffusion to lower atomic layers along the intersecting dislocation helix formed during epitaxial growth.

Since its development, the scanning tunneling microscope[3] (STM) has proven to be a unique tool for resolving the atomic-scale realm of matter. As opposed to the traditional diffraction methods, STM is the technique of choice to directly reveal disorder and imperfections on surfaces. Static images of dislocations emerging on surfaces have been published in the past.[4,5] With the development of very stable, thermal-drift compensated STMs that allow for fast scanning, it has become possible from STM movies to follow morphological changes on surfaces dynamically in real time. Examples of such research include the investigation of Brownian motion of adatom and vacancy islands towards thermal equilibrium,[6–8] partial-edge dislocations in a single-monolayer film,[9] and thermal fluctuations of equilibrium step-edge structures.[10–12]

In this paper, we follow the dynamics of a helical step emerging at the intersection of a screw dislocation with the surface with fast-scanning STM. A helical step is an energetically unfavorable, nonequilibrium situation. We discuss the influence of the dislocation on the evolution of the helical step towards equilibrium, i.e., a straight step. Furthermore, we describe changes to the evolution due to a coalescence event of the step with a vacancy island.

The STM measurements are performed on a single-crystal Ag(111) surface in a UHV system (base pressure 5×10^{-11} mbar) equipped with the home-built, fast-scanning, variable-temperature Aarhus STM as well as the standard surface science techniques for sample preparation and characterization.[13] The Ag(111) surface is cleaned by several sputtering-annealing cycles. Vacancy islands and helical steps are created by 1 keV-Ne$^+$-sputtering at room temperature with an ion current of 1 μA. Special care is taken to ensure that the STM data are not influenced by the imaging process.[7]

The intersection of a screw dislocation with the Ag(111) surface leads to the formation of a monatomic step (Fig. 1). Atomic resolution shows that the step is oriented in the $\langle 110 \rangle$ direction, as expected for annealed dislocations on a Ag(111) surface, since the {111} planes are the primary gliding planes in a fcc lattice, and the intersection of a {111} plane on the (111) surface follows a $\langle 110 \rangle$ direction. The type of dislocation observed here is described by the Burgers vector $\mathbf{b} = 1/2[110]a$, with the lattice constant a. Heidenreich and Shockley[14] showed that it is energetically favorable for the displacement of $\mathbf{b} = 1/2[110]a$ to occur in two steps characterized by the Burgers vectors, $\mathbf{b_1} = 1/6[12\bar{1}]a$ and $\mathbf{b_2} = 1/6[211]a$, which obey $\mathbf{b} = \mathbf{b_1} + \mathbf{b_2}$. This is energetically favorable, because Frank's rule,[15] i.e., $\mathbf{b_1}^2 + \mathbf{b_2}^2 < \mathbf{b}^2$, is fulfilled here. The first vector displaces the atoms to the hcp hollow sites, thereby introducing a stacking fault in the crystal, perpendicular to the (111) plane, of $\frac{1}{3}$ or $\frac{2}{3}$ of the total step height. The second vector displaces the atoms to the neighboring fcc hollow site. Consequently, the total step height, $h = 0.236$ nm, of the Ag(111) surface is reached. The reduced step height between the partials is in agreement with this assignment.[5] The two partials of the dislocation are separated by ~ 6 nm. The distance is larger than the bulk splitting distance due to the influence of the surface,[5] the reason for this being that the screw dislocations have a lower elastic energy than the edge dislocations and that the break in the translational symmetry at the surface allows the partials to reorient to obtain more screw character and thus reduce their energies.

Only the short part of the step between the partials is oriented along the $\langle 110 \rangle$ direction (Fig. 1), and this straight part ends with the emergence of the second partial. The remaining part of the surface dislocation deviates from the
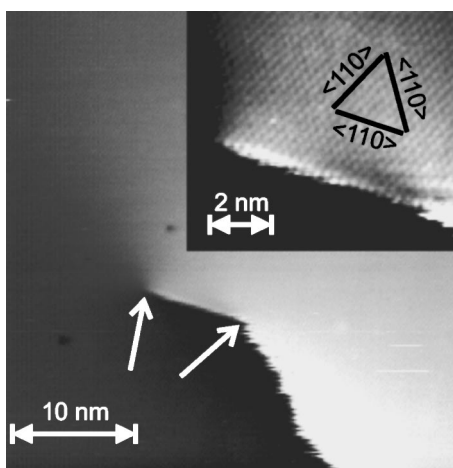
FIG. 1. STM image of the intersection of a screw dislocation with the surface. Between the two partials (marked by white arrows), the positions of the atoms do not change within half an hour; beyond the second partial (i.e., right of the right arrow), the step shows the frizziness expected for Ag(111) at this temperature (Refs. 10 and 11). $U = -0.221$ V, $I = 0.07$ nA, $T = 330$ K; the inset shows the atomic resolution image of the region between the partials, $U = -0.221$ V, $I = 0.12$ nA.

close-packed $\langle 110 \rangle$ direction and shows in STM movies (see Ref. 16) a characteristic frizziness, indicating step fluctuations due to frequent adatom rearrangements at the step.[10,17] The region between the two partials, however, shows no atom rearrangement, as is verified in the atom-resolved STM movies of this region at 330 K, indicating that the steps between partials have a higher step stiffness than regular steps, and that the dislocation itself is immobile at the temperature of the measurement (330 K).

Gently sputtering the surface at room temperature with 1 keV-Ne$^+$ ions (1 μA) leads to a nonequilibrium configuration. The step emerging from the screw-dislocation intersection in Fig. 2 forms a helix. Artificially created nonequilibrium nanostructures on Ag(111) have been shown to
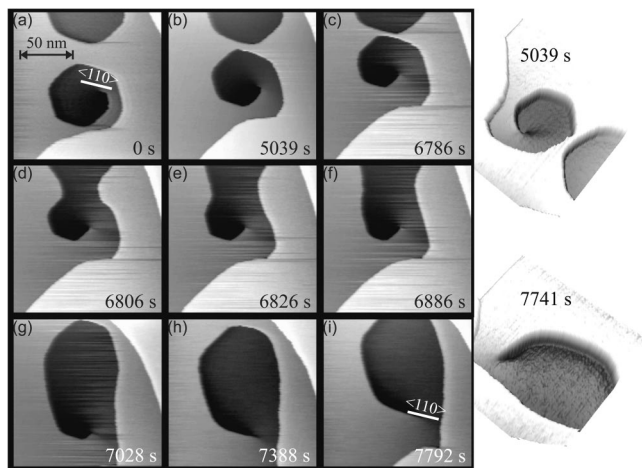
FIG. 2. Snapshots from a movie containing 385 images with one image recorded every 20 s. $U = 2.13$ V, $I = 0.1$ nA, $T = 320$ K. For a better impression of step height changes two 3D images are shown in the right part of the image.

evolve towards thermal equilibrium structures at room temperature on the time scale of hours.[6,7] For the helix in Fig. 2 to evolve towards an equilibrium configuration (Fig. 1), the helical step has to wander around the immobile Shockley partials. In Fig. 2, we show the first passing of the partials at 320 K from right to left in the image. The motion requires a change in the relative position of the partials with respect to the step. In the beginning the step emerges from the right-hand side of the partials [left-hand side in the three-dimensional (3D) plot]. After a time lapse of 6786 s the step emerges from the other side of the intersection (right-hand side in the 3D plot).

We choose to show this particular example here, because a coalescence event with a vacancy island (see Ref. 16), which is also produced during sputtering due to the assembly of vacancies, sheds further light on the development towards equilibrium of nonsymmetric nanostructures. Further evolution towards equilibrium without this coalescence event repeats the sequence observed earlier within a much longer time scale, thus yielding no additional information. The next passing (without coalescence) is estimated to be in approximately 14 h.

In order to analyze the dislocation dynamics quantitatively, we measure the lengths of the angular helix sides and the angles between them, as depicted in Fig. 3(a), as well as the step heights at the corners of the helix. As exemplified for ϕ_3 and ϕ_4, the angles between the straight edges of the helix are comparable to those for the vacancy islands on the same surface [Fig. 3(b)], indicating that on a large scale the crystallographic order can be only slightly disturbed, if at all. The angles do not change unless the neighboring segment has almost vanished, upon which the value of the next angle is smoothly approached [Fig. 3(b)], in accordance with rounded corners between steps of different crystallographic orientations.

The evolution of the total step length [Fig. 3(c)] suggests the existence of five qualitatively different time regimes between 0 and 6004 s (I), 6004 and 6807 s (II), 6807 and 7270 s (III), 7270 and 7571 s (IV), and 7571 and 7792 s (V). A thorough analysis of the STM movie[16] reveals that these regimes are separated by the following events: (i) At $\sim$6000 s the step passes from one side of the partials to the other one, during which l_2 disappears. The passing of the partials is shown in more detail in Fig. 4. At 5943 s, the step is about in the middle between the two partials. A final passing from another movie at slightly higher temperature is also shown. The first three images shown suggest that the passing is unidirectional. However, three images at a later time show that in this slow evolution there are fluctuations along the step between the partials. (ii) At $\sim$6800 s the helix coalesces with a vacancy island [cf. Fig. 2(d)]. (iii) At $\sim$7300 s l_3 disappears and the step is aligned with the partial's direction [cf. Fig. 2(h)] because l_4 and l_1 are parallel. (iv) At $\sim$7600 s the influence of the coalescence event vanishes with the last part of the step with positive curvature. Table I summarizes the slopes of the linear fits to the experimental data in the different regions [see Figs. 3(d) and 3(e)].

In region I, the total length of the step segments [$l_{ges} = \Sigma_{i=1}^5 l_i$, Fig. 3(c)] decreases with an average rate of 5.5 pm/s. It should be noted, however, that the slope is not
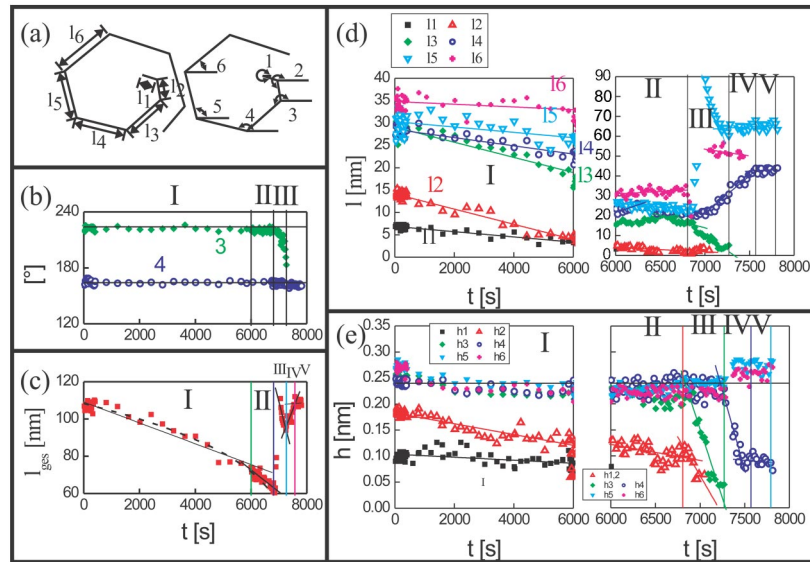
FIG. 3. (Color online) Evolution of the helix: (a) Sketch indicating the angles and lengths measured; h_i is measured at ϕ_i. (b) Angles ϕ_3 (filled diamonds) and ϕ_4 (open circles). The solid lines represent the angles between the step segments of a vacancy island on the same surface. (c–h) Symbols: experimental values, solid lines; linear fits, dashed line; power-law fit (see text). (c) Total step length $l = \Sigma_{i=1}^{5} l_i$. (d) Length of step segments. (e) Step height in corners of the helix. Note that in (d) and (e) the time scales are different in the two graphs. The fluctuations around the mean values of the lengths are largely due to Brownian motion, which has been analyzed for this surface at even lower temperature (Ref. 11). For region I a reduced data set is shown only.

linear. Fitting the data with the expression $a\,(b-t)^c$, results in a decay exponent of $c = 0.26 \pm 0.05$, which is close to the exponent found in Ref. 18 for the final stage of vacancy-island reshaping after a coalescence event.

The step segments decrease with different rates. Besides l_1, for which the limit imposed by the equilibrium separation of the two partials is reached, the decay is the slower, the larger the segment and the further away it is from the intersection. As a result the (half) hexagon formed by l_3 to l_6, which is close to symmetric in the beginning of the measurement, is deformed to $l_3 < l_4 < l_5 < l_6$. This may be explained by the relative position of the partials to the center of the hexagon; the local curvature near the partials increases, while the hexagon rearranges, bringing the partials closer to the center.

For the reshaping of the two-dimensional vacancy islands during coalescence we have shown previously[18] that the final

relaxation to the equilibrium shape varies strongly with the island size (3rd to 4th power of the island diameter). This is close to the exponent of 0.25 found above in region I. In Ref. [18], we found that the smaller the islands, the faster they relax, which can explain the different rates between step segments of different lengths.

The fact that the step approaches the region of the partials manifests itself in a change in height. We find that h_2 decreases continuously while approaching the constant h_1 of $\frac{1}{3}$ h, where $h = 0.236$ nm is the full step height of Ag(111). Close to 6000 s, h_2 and h_1 have the same height [Fig. 3(e)]. It should be mentioned that the variation in h_1 is within the experimental uncertainty; i.e., h_1 is constant.

After the step passes the partials, the behavior described above changes significantly (region II). The total step length now decreases almost twice as fast [Fig. 3(c)] and the height $h_{1,2}$ decreases with a triple rate [Fig. 3(e)]. However, not all
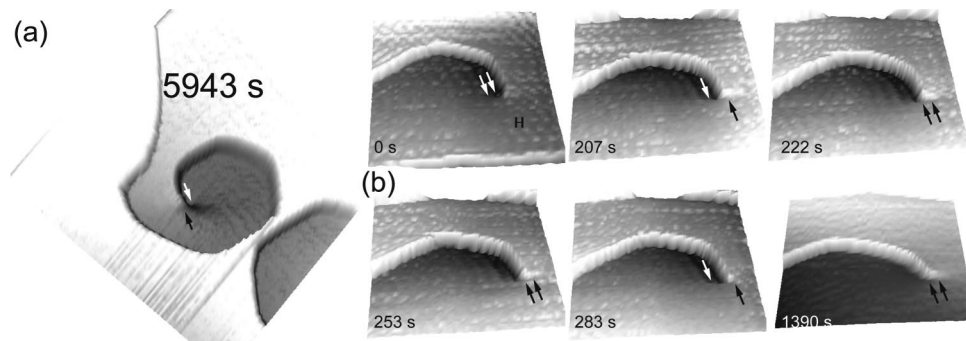

FIG. 4. 3D representation of the passing of the full-height step along the reduced-step height between the emergence of partials. The arrows point to these partials: (a) From the movie shown in Fig. 2 at 5943 s. (b) Snapshots from a movie containing 92 images with one image recorded every 15 s. $U = 2.13$ V, $I = 0.02$ nA, $T = 343$ K and 170 nm $\times$ 176 nm.

TABLE I. Slopes in pm/s of linear fits to the experimental data in Fig. 3.

Region pm/s	l_{ges}	l_2	l_3	l_4	l_5	l_6	h_1	h_2	h_3	h_4	h_5
I	−5.5	−1.7	−1.7	−0.9	−0.6	−0.3	−0.0029	−0.0104	0.0	0.0	0.0
II	−11.8	−2.2	+6.8 / −12.5	+15.0 / −5.9	−4.1	+2.4		−0.0373	0.0	0.0	0.0
III	−85.0	−2.2	−31.1	+38.6	−136	−6.8		−0.3570	−0.6400	0.0	0.0
IV	+38.2			+38.6	−2.7	+2.7				−0.7370	0.0
V	+1.1			+2.8		+2.7				−0.0188	0.0

segments decrease immediately. The smaller segments initially increase in length. In contrast, we see an equilibration which is very similar to the equilibration of the vacancy islands.[18] Remarkable here and throughout the measurement are the rather sharp changes in slope for the length evolution. At the end of region II, the situation is similar to the one in region I, where the segments (besides l_2) decrease at a lower rate, the longer they are and the further away they are from the intersection.

It is interesting to note the difference between regions I and II. In region I, the decay rate depends on length, whereas in region II, the step lengths try to approach each other. The difference, in evolution shows that the equilibrium structure of a helical step is different, depending on the relative orientation of the steps to the partials. The increased rate and the slope inversion demonstrate the influence of a seemingly local situation (relative position of the step to the partials) on the evolution and the atomic motion over distances of several tens of nanometers, due to the fast diffusion of atoms along the step edge that are important for the mass transport (see below).

Following the coalescence event (region III), the total length decreases more than 1 order of magnitude faster than in region I due to the additional supply of adatoms from the highly curved bumps formed upon coalescence.[18] E.g., l_5 decreases more than 30 times faster than before the coalescence event. The change in slope of l_4 observed after more than 100 s is related in time to the end of the decay of the coalescence-induced bump at the step edge. The acceleration of the evolution due to the increased number of adatoms supplied by the coalescence event is also apparent in the increased decay rates of $h_{1,2}$ (1 order of magnitude) and h_3 [double rate of h_2, Fig. 3(e)]. The only significant change which is observed after the disappearance of l_3 (region IV) is that h_4 decreases with a rate similar to the former decrease of h_3.

The fast coalescence-induced changes stop with the disappearance of the last part of the step with a positive curvature. A new dynamic equilibrium is thus reached in region V after fast changes for a time span of 780 s.

The decrease in the long axis $[\approx l_5 + (l_6 + l_4)/2]$ of the structure formed upon the coalescence decreases linearly as found in a shape analysis. This is different from the exponential decrease of the island's long axis after island coalescence on the same surface (for vacancies see Ref. 18, for adatoms see Ref. 19), which has a decay time of the order of minutes already at room temperature.

Monatomic steps in STM movies recorded at room temperature are well known to appear frizzy and to fluctuate around a mean value due to the fast rearrangement of step adatoms at the step.[17] This equilibrium process manifests itself here in an apparent scatter of the data around mean values. For a closed step (i.e., an adatom or a vacancy island), the fluctuations result in a Brownian motion of the island as a whole over the surface (e.g., Ref. 11). In contrast, in the present nonequilibrium situation, the step adatom motion leads to a change in shape, i.e., a net flux of adatoms. As the atomic motion is not revealed in the STM movies, we cannot directly tell whether the adatoms diffuse over the terrace, and thus the observed changes in the shape of the dislocations are due to the detachment-reattachment mechanism or whether the adatoms diffuse along the step edge. The latter process seems to be more likely, because on Ag(111) the Brownian motions of the vacancy islands,[20] the coalescence of the vacancy island,[18] and the step fluctuations of the unpinned steps[17] are dominated by step-edge diffusion. In order to quantify this supposition, on the one hand we compare the changes observed here to the decay rate of adatom islands, and on the other hand we compare the changes to the filling of the vacancy islands. The two processes differ in the sense that in the latter case the diffusing adatoms must overcome the so-called Ehrlich-Schwoebel barrier,[2] which slows down the evolution towards thermal equilibrium in the case of vacancy-island filling. We estimate that around 8000 atoms have been added to the step from l_1 to l_6 within the first 6000 s. From our previous studies we know that the filling of a vacancy island by this number of atoms would take approximately 90 h at room temperature.[7] Consequently, even at 320 K an adatom motion mechanism involving the Ehrlich-Schwoebel barrier cannot be responsible for the observed changes in the dynamics of dislocations. The shrinking of an adatom island by 8000 atoms would take around 60 000 s at room temperature,[7] and can thus be estimated to take 10 000 s at the measurement temperature. We therefore tentatively conclude that a combination of the detachment-reattachment mechanism and a supply of adatoms along the step edge is responsible for the observed behavior in regions I and II. The influence of the decay rate by the passing of the partials demonstrates that the region acts as a sink for the atoms from the terrace, in contrast to the assumption in Ref. 21, and thus provides a supply of atoms via step diffusion.

We can compare the dynamics of the dislocation after the coalescence event has occurred to the results we find for the reshaping of the vacancy islands after their coalescence, where we identify the diffusion along the step to be the

dominating mechanism.[18] The relaxation of a vacancy island of a similar size should take around 200 s at room temperature. After the coalescence event the attachment-detachment mechanism does not supply enough atoms to explain the observed very fast changes. The coalescence event leads to convex steps which increase the steps' chemical potential, and which consequently accelerate the evolution towards equilibrium. From the rates, this is the only possible mechanism. The evolution, however, is slowed down by the existence of the partials, which are immobile at the temperature of the measurement. Instead of an exponential decay, we find a linear decay of the long axis of the elongated structure.

In conclusion, we have studied the atomic-scale dynamics of a helical step emerging at the intersection of a bulk dislocation on a Ag(111) surface at room temperature. The difficulty of passing this region slowed down the evolution towards equilibrium, as compared to the situation afterwards, where the step was still fixed at one end due to the dislocation. The dislocation lead to a long-range perturbation of step-edge diffusion. A coalescence event gave an additional supply of adatoms which accelerated the evolution accordingly. Needless to say, it would be highly desirable to simulate these processes in order to gain insight into the reorientation of the step on an atomistic level, especially in the region of reduced step height. Hopefully our studies will help stimulate such work in the future.

[1] E. Nadgornyi, *Dislocation Dynamics and Mechanical Properties of Crystals* (Pergamon, Oxford, 1988).

[2] G. Ehrlich and F. G. Hudda, J. Chem. Phys. **44**, (1966) 1039; R. L. Schwoebel and E. J. Shipsey, J. Appl. Phys. **37**, 3682 (1966).

[3] G. Binnig and H. Rohrer, Surf. Sci. **152/153**, 17 (1985).

[4] J. F. Wolf and H. Ibach, Appl. Phys. A: Solids Surf. **52**, 218 (1991); J. F. Wolf, B. Vicenzi, and H. Ibach, Surf. Sci. **249**, 233 (1991); A. Samsavar, E. S. Hirschorn, T. Miller, F. M. Leibsle, J. A. Eades, and T.-C. Chiang, Phys. Rev. Lett. **65**, 1607 (1990); G. Cox, D. Szynka, U. Poppe, K. H. Graf, K. Urban, C. Kisielowski-Kemmerich, J. Kruger, and H. Alexander, *ibid.* **64**, 2402 (1990); M. Schmid, A. Biedermann, H. Stadler, and P. Varga, *ibid.* **69**, 925 (1992); J. Jacobsen, L. Pleth Nielsen, F. Besenbacher, I. Stensgaard, E. Lægsgaard, T. Rasmussen, Z. Gai, Y. He, X. Li, J. F. Jia, and W. S. Yang, Surf. Sci. **365**, 96 (1996); J. de la Figuera, M. A. Gonzalez, R. Garcia-Martinez, J. M. Rojo, O. S. Hernan, A. L. Vazquez de Parga, and R. Miranda, Phys. Rev. B **58**, 1169 (1998); O. Rodriguez de la Fuente, J. A. Zimmerman, M. A. Gonzalez, J. de la Figuera, J. C. Hamilton, W. W. Pai, and J. M. Rojo, Phys. Rev. Lett. **88**, 036101 (2002).

[5] J. Christiansen, K. Morgenstern, J. Schiøtz, K. W. Jacobsen, K.-F. Braun, K.-H. Rieder, E. Lægsgaard, and F. Besenbacher, Phys. Rev. Lett. **88**, 206106 (2002).

[6] K. Morgenstern, G. Rosenfeld, and G. Comsa, Phys. Rev. Lett. **76**, 2113 (1996).

[7] K. Morgenstern, G. Rosenfeld, E. Lægsgaard, F. Besenbacher, and G. Comsa, Phys. Rev. Lett. **80**, 556 (1998).

[8] K. Morgenstern, E. Lægsgaard, I. Stensgaard, and F. Besenbacher, Phys. Rev. Lett. **83**, 1613 (1999); D. R. Peale and B. H. Cooper, J. Vac. Sci. Technol. A **10**, 2210 (1992); J.-M. Wen, J. W. Evans, M. C. Bartelt, J. W. Burnett, and P. A. Thiel, Phys. Rev. Lett. **76**, 652 (1996); J. B. Hannon, C. Klünker, M. Giesen, H. Ibach, N. C. Bartelt, and J. C. Hamilton, *ibid.* **79**, 2506 (1997); A. Ichimiya, Y. Tanaka, and K. Ishiyama, Surf. Sci. **386**, 182 (1997); W. W. Pai, A. K. Swan, Zh. Zhang, and J. F. Wendelken, Phys. Rev. Lett. **79**, 3210 (1997); M. Giesen, G. Schulze Icking-Konert, and H. Ibach, *ibid.* **80**, 552 (1998); W. W. Pai, J. F. Wendelken, C. R. Stoldt, P. A. Thiel, J. W. Evans, and D.-J. Liu, *ibid.* **86**, 3088 (2001).

[9] A. K. Schmid, N. C. Bartelt, J. C. Hamilton, C. B. Carter, and R. Q. Hwang, Phys. Rev. Lett. **78**, 3507 (1997).

[10] M. Poensgen, J. F. Wolf, J. Frohn, M. Giesen, and H. Ibach, Surf. Sci. **274**, 430 (1992).

[11] K. Morgenstern, G. Rosenfeld, B. Poelsema, and G. Comsa, Phys. Rev. Lett. **74**, 2058 (1995).

[12] L. Kuipers, M. S. Hoogeman, and J. W. M. Frenken, Phys. Rev. Lett. **71**, 3517 (1993); W. W. Pai, N. C. Bartelt, and J. E. Reutt-Robey, Phys. Rev. B **53**, 15 991 (1996).

[13] E. Lægsgaard, F. Besenbacher, K. Mortensen, and I. Stensgaard, J. Microsc. **152**, 663 (1988); F. Besenbacher, Rep. Prog. Phys. **59**, 1737 (1996).

[14] R. O. Heidenreich and W. Shockley, *Rep. Conference Strength of Solids, Bristol, 1947* (The Physical Society, London, 1948), p. 57.

[15] F. C. Frank, Physica (Utrecht) **15**, 131 (1949).

[16] http://www.fkp.uni-hannover.de/~morgenstern/dislocationmovies.html or http://www.phys.au.dk/camp/movies/karina.htm

[17] M. Giesen, Prog. Surf. Sci. **68**, 1 (2001).

[18] M. Eßer, K. Morgenstern, G. Rosenfeld, and G. Comsa, Surf. Sci. **402–404**, 341 (1998).

[19] K. Morgenstern, Phys. Status Solidi B **242**, 773 (2005).

[20] D. C. Schlößer, K. Morgenstern, L. K. Verheij, G. Rosenfeld, F. Besenbacher, and G. Comsa, Surf. Sci. **465**, 19 (2000).

[21] N. Quaas, M. Wenderoth, and R. G. Ulbrich, Surf. Sci. **550**, 57 (2004).